INTERNATIONAL JOURNAL FOR NUMERICAL METHODS IN ENGINEERING
Int. J. Numer. Meth. Engng 2004; **61**:1310–1331 (DOI: 10.1002/nme.1106)

Analytic preconditioners for the electric field integral equation

X. Antoine[1,*,†], A. Bendali[2] and M. Darbas[2]

[1]*MIP (UMR 5640), UFR MIG, Université Paul Sabatier, 118, route de Narbonne, 31062 Toulouse Cedex, France*
[2]*Département de Génie Mathématique, INSA, MIP UMR-5640, Complexe Scientifique de Rangueil, 31077, Toulouse Cedex 4, France*

SUMMARY

Since the advent of the fast multipole method, large-scale electromagnetic scattering problems based on the electric field integral equation (EFIE) formulation are generally solved by a Krylov iterative solver. A well-known fact is that the dense complex non-hermitian linear system associated to the EFIE becomes ill-conditioned especially in the high-frequency regime. As a consequence, this slows down the convergence rate of Krylov subspace iterative solvers. In this work, a new analytic preconditioner based on the combination of a finite element method with a local absorbing boundary condition is proposed to improve the convergence of the iterative solver for an open boundary. Some numerical tests precise the behaviour of the new preconditioner. Moreover, comparisons are performed with the analytic preconditioner based on the Calderòn's relations for integral equations for several kinds of scatterers. Copyright © 2004 John Wiley & Sons, Ltd.

KEY WORDS: electromagnetism; integral equation; analytic preconditioners; Krylov subspace iterative solver

1. INTRODUCTION

Boundary integral equations are well-known for being efficient to compute the solution to a high-frequency electromagnetic scattering problem [1, 2]. Their principle is based on an equivalent writing of the initial boundary value problem in an open-region as an equation set on the *finite* surface of the scatterer. Several integral formulations exist and are in a certain sense equivalent from a theoretical point of view. For the scattering problem by an open surface, it is admitted that the electric field integral equation (EFIE) provides a suitable formulation and yields accurate results [2]. Despite their efficiency, integral equations have the drawback of being defined by a non-local integro-differential operator and lead to the solution of a dense complex non-hermitian linear system. When the size n (representing the number of degrees of freedom of the discretization) becomes large especially for high-frequency problems, the

*Correspondence to: X. Antoine, MIP (UMR 5640), UFR MIG, Université Paul Sabatier, 118, route de Narbonne, 31062 Toulouse Cedex, France.
†E-mail: antoine@mip.ups-tlse.fr

Received 22 July 2003
Revised 20 January 2004
Accepted 11 February 2004

Published online 31 August 2004

resolution of the system by a direct solver is not realistic and requires $\mathcal{O}(n^3)$ operations. Since the introduction of the fast multipole method (FMM) in the middle of the eighties by Rokhlin [2, 3], the solution is generally reached with the help of a Krylov subspace iterative solver [4, 5] (e.g. CGS, BiCGSTAB, GMRES, QMR, etc.). The computational cost is then of the order of $\mathcal{O}(n^{\text{iter}}n^2)$, where n^{iter} designates the number of iterations needed to obtain a satisfactory approximate solution. The complexity $\mathcal{O}(n^2)$ issued from the evaluation of matrix–vector (MV) products can be efficiently reduced to $\mathcal{O}(n \log n)$ by the FMM [2, 6]. In conjunction to this improvement, one can also speed up the algorithm by diminishing the cost n^{iter}. This last parameter is in fact related to the condition number of the linear system. Integral equations are well-known for being generally ill-conditioned [2, 4, 7] and preconditioners are employed to improve the convergence rate of the iterative solver. Among the most widely used approaches and without being exhaustive, let us cite for instance the methods based on the splitting of operators [4, 8] or the algebraic preconditioners (ILU, SPAI, LU, etc.) [9–11].

Recently, Christiansen and Nédélec [12, 13] have proposed a new class of analytic preconditioners for both the Helmholtz and Maxwell equations. Their construction uses the works of Steinbach and Wendland [14] who achieve some preconditioners based on the integral relations of Calderòn. This permits to develop an explicit pseudo-inverse integral operator of the EFIE for both the TM and the TE polarizations. One crucial advantage of this approach over previous preconditioners is that the underlying physics of the scattering problem is implicitly taken into account. One of the drawbacks is that the application of the preconditioner doubles the number of matrix–vector products per iteration. We propose in this paper the construction of an implicit sparse preconditioner based on a finite element formulation of a local boundary value problem involving an artificial boundary condition. The resulting preconditioner hence requires at each step the resolution of a small sparse complex symmetric linear system with a computational cost of the order of $\mathcal{O}(n)$. As the Caldèron's preconditioners, these new preconditioners incorporate the physical properties of the problem to solve.

The plan of the paper is the following. In Section 2, we briefly review the EFIE formulations for the two-dimensional scattering problem of a TM or TE polarized incident wave by a perfectly conducting body. In Section 3, we recall some recent results of Chew and Warnick [2, 7] concerning the high-frequency analysis of the spectrum of the EFIE for the flat strip. This gives a better comprehension of what kind of parameters influence the convergence rate of a Krylov iterative solver applied to the EFIE. In Section 4, after some recalls about the Caldèron's integral preconditioners, we develop a new approach for the construction of a local implicit analytic preconditioner for the EFIE. It consists in solving a local approximate scattering problem to construct an approximate sparse representation of the operator related to the EFIE under consideration. The method is implemented in some Krylov iterative solvers and its performance is numerically analysed for the scattering problem by a screen. Some comparisons are provided for both the mass matrix and the Caldèron's preconditioners. In Section 5, we give an extension of the method in the case of a resonant rectangular cavity and improve the efficiency of the preconditioner by presenting a partitioning of the domain for a large-size electrical scatterer. Finally, a conclusion is drawn in Section 6.

2. THE EFIE FORMULATION

Let us consider a smooth bounded domain $\Omega^- \subset \mathbb{R}^2$ with a smooth open boundary $\Gamma = \partial\Omega^-$ and let $\Omega^+ = \mathbb{R}^2 \setminus \overline{\Omega^-}$ be the associated exterior domain of propagation. If u^{inc} designates

an incident wave defined by a wavenumber $k = 2\pi/\lambda$, where λ is the wavelength, then the scattered field u in the domain Ω^+ is solution to the exterior boundary-value problem (BVP) (see e.g. Reference [1]),

$$\begin{gathered} \text{Find } u \text{ such that} \\ \Delta u + k^2 u = 0 \quad \text{in } \Omega^+ \\ u = g \text{ or } \partial_{\mathbf{n}} u = g \quad \text{on } \Gamma \\ \lim_{|x|\to+\infty} |x|^{1/2} \left(\nabla u \cdot \frac{x}{|x|} - \mathrm{i}ku \right) = 0 \end{gathered} \tag{1}$$

This BVP models the scattering of a TM-polarized (Dirichlet boundary condition with $g = -u^{\text{inc}}$) or a TE-polarized (Neumann boundary condition with $g = -\partial_{\mathbf{n}} u^{\text{inc}}$) incident wave by a perfectly conducting cylinder of transverse section Ω^-.

One of the main difficulties arising in the numerical solution of the BVP (1) is linked to the *unbounded* character of the exterior domain Ω^+. One possible solution consists in reducing the initial problem (1) to an equivalent integral equation set on the *finite* surface Γ. Here, we consider the EFIE which is known for being efficient for the scattering problem by an open surface. More precisely, let us define the densities,

$$p = [\partial_{\mathbf{n}} u]_\Gamma \quad \text{and} \quad \phi = [u]_\Gamma \tag{2}$$

where $v^\pm$ represents the restriction to $\Omega^\pm$ of a function v defined in $\mathbb{R}^2 \setminus \Gamma$ and $[v] = v^- - v^+$ is the jump of a field v across Γ. We denote by G the free-space Green's function in $\mathbb{R}^2$ given by,

$$G(x, y) = \frac{i}{4} H_0^{(1)}(k|x - y|), \quad x \neq y \tag{3}$$

where $H_0^{(1)}$ is the zeroth-order Hankel function of the first kind. The TM–EFIE formulation is

$$Vp(x) = g(x), \quad x \in \Gamma \tag{4}$$

where V is the single-layer potential defined by

$$Vp(x) = \int_\Gamma G(x, y) p(y) \, \mathrm{d}\Gamma(y), \quad x \in \Gamma \tag{5}$$

For the TE case, we get

$$N\phi(x) = g(x), \quad x \in \Gamma \tag{6}$$

where N is the normal derivative of the double-layer potential defined by

$$N\phi(x) = -\partial_{\mathbf{n}(\mathbf{x})} \int_\Gamma \partial_{\mathbf{n}(\mathbf{y})} G(x, y) \phi(y) \, \mathrm{d}\Gamma(y), \quad x \in \Gamma \tag{7}$$

3. ASYMPTOTIC SPECTRAL ANALYSIS OF THE EFIE FOR THE SCREEN

The boundary element approximation of the EFIE generates a dense non-hermitian complex-valued matrix $[Z]$, where Z is the integro-differential operator defining the EFIE according to the polarization. If one wants to solve the associated linear system by a Krylov subspace iterative solver, it becomes central to have a better understanding of the influence of both the physics and geometrical and finite element approximations over the number of iterations n^{iter} needed to reach a sufficiently accurate solution. This allows to analyse which parameters must be handled to develop some efficient continuous or discrete preconditioners. This is particularly crucial when the size of the obstacle becomes large compared to the wavelength λ (high-frequency regime). To highlight the origin of the deterioration of the condition number of the EFIE, we recall some results recently obtained by Chew and Warnick [7] concerning the spectral analysis of the EFIE when Γ is a screen.

We consider here a flat screen $\Gamma = [-d/2, d/2]$. We designate by h the uniform mesh size of Γ arising in the discretization of the TM–EFIE by a linear boundary element method. Let us, respectively, denote by $D = d/\lambda$ and $n_\lambda = \lambda/h$ the dimensionless length of the strip in wavelengths and the number of nodes per wavelength. The operator V is non-normal and non-hermitian. A possible issue to study the spectral decomposition of V would be to split it into two terms: its static part and a corrective compact perturbation. However, for high frequencies ($D \to +\infty$), this perturbation becomes dynamical and hence penalizes the convergence rate of the involving iterative solver. To overcome this problem, Chew and Warnick propose a specific treatment which consists in splitting V into a normal operator and the complementary non-normal correction. Following their approach, they prove that the normal part is linked to the physical optics scattering approximation and yields a correct representation of the spectrum of V. Let us denote by ξ the Fourier covariable of the anticlockwise directed curvilinear abscissa s along Γ. Then, if we consider a low-frequency propagative mode ($|\xi| < k$), Chew *et al.* show that the associated eigenvalue has a behaviour close to $\mathrm{i}(2k)^{-1}$ and lies on the pure imaginary axis. Now let us notice that the evanescent modes (exponentially decaying) have a spatial frequency $|\xi|$ which tends toward $+\infty$. Then, following [7], it can be proved that the eigenvalue associated to a high spatial frequency ξ can be approximated by $(2|\xi|)^{-1}$ and tends toward zero on the real axis. All these results can be linked from a mathematical point of view to the concept of principal symbol of a pseudodifferential operator [15]. However, we do not develop this relation with the work of Chew and Warnick and refer to Reference [16] for further details. Finally, the last estimate of the eigenvalues is obtained for the modes such that $|\xi| \approx k$. These frequencies characterize the surface modes and reproduce the strong coupling between the evanescent and propagative rays through a complex eigenvalue which depends on the geometry and frequency λ. Chew and Warnick [7] provide an estimate of this eigenvalue for the screen showing that it behaves like $\sqrt{2}\lambda(1+i)D^{1/2}/(6\pi)$ in the high-frequency domain $D \to +\infty$. Then, from a continuous and discrete point of view, this eigenvalue provides a good estimate of the largest eigenvalue $\Lambda_M(V)$ and $\Lambda_M([V])$ of, respectively, the integral operator V and matrix $[V]$

$$\Lambda_M(V) = \Lambda_M([V]) \simeq \frac{\sqrt{2}\lambda}{6\pi}(1+i)D^{1/2} \tag{8}$$

For $D \to \infty$, it behaves like the square root of the size of the scatterer expressed in wavelengths units. Hence, it constitutes a specific parameter of the problem independent of the discretization

scheme and therefore cannot be reduced without the use of an appropriate preconditioner which integrates the creeping rays contribution. As previously mentioned, the infinite sequence of eigenvalues of the operator V tends toward zero when $|\xi| \to +\infty$ yielding an infinite conditioning of V. Now, let us consider the finite space approximation based on equally spaced linear finite elements. The selection of the number of Fourier modes $2[|\xi|/k] + 1$ is fixed by the Nyquist–Shannon sampling theorem which states that samples spaced apart by h exactly represent functions whose shortest wavelengths are $4h$. However, since we rather represent the inverse Fourier transform corresponding to the superposition of plane waves, we relax $4h$ by the weaker Nyquist condition $2h$ yielding

$$\frac{2\pi}{|\xi|} \approx 2h \iff \frac{|\xi|}{k} \approx \frac{n_\lambda}{2} \tag{9}$$

Therefore, the smallest eigenvalue $\Lambda_m([V])$ of $[V]$ is given by the sampling of the cutoff value of the spectrum of V at the Nyquist frequency,

$$\Lambda_m([V]) \simeq \frac{\lambda}{2\pi n_\lambda} \tag{10}$$

This last estimate is always satisfied for any scatterer. From these approximations, we have the following estimate of the condition number $\kappa([V])$ associated to the matrix $[V]$:

$$\kappa([V]) \simeq \tfrac{2}{3}\, n_\lambda D^{1/2} \tag{11}$$

Considering the TE-polarization case, we can see that N is a hypersingular integral operator. Proceeding in a similar way as for the TM case, we get that the largest eigenvalue at the Nyquist frequency is given by

$$\Lambda_M([N]) = \frac{\pi n_\lambda}{2\lambda} \tag{12}$$

The smallest eigenvalue comes from the surface wave mode and may be approximated [7] by

$$\Lambda_m([N]) \simeq \frac{\sqrt{2}(1-i)D^{-1/2}}{\lambda} \tag{13}$$

As a consequence, an estimate of the condition number of $[N]$ is

$$\kappa([N]) = \frac{\pi}{4}\, n_\lambda D^{1/2} \tag{14}$$

4. A LOCAL ABC–FEM-BASED PRECONDITIONER FOR THE EFIE

This section is devoted to the construction of some suitable preconditioners with the aim of overcoming at least partially the difficulties observed during the preceding section. In a first part, we recall the idea of the integral preconditioners based on the Caldèron's formulae and show in the case of the screen their numerical capacity of involving the underlying physics. Next, we propose a new implicit sparse preconditioner for both the TM and TE polarizations. The basic idea is based on the localization of the preconditioner by using the Helmholtz partial differential equation in a fine layer surrounding the strip and truncating the open region with a simple local artificial boundary condition.

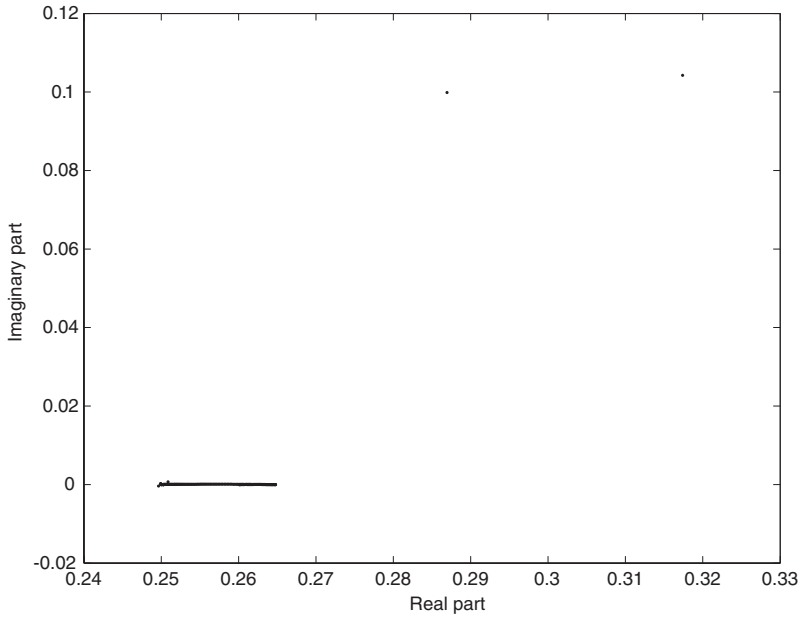

Figure 1. Discrete spectrum of the linear finite element matrix $[C]$ ($n_\lambda = 20$, $D = 10$ and $d = 2$).

4.1. The integral preconditioners based on the Caldèron's formulae

One of the motivations when one wants to construct a suitable preconditioner is to obtained a cheap approximation of the inverse of the operator defining the equation to solve. Steinbach and Wendland [14], propose to use the following Caldèron's relations satisfied in the case of a closed surface:

$$VN = I/4 - K^2 \quad \text{and} \quad NV = I/4 - (K^{\mathrm{T}})^2 \tag{15}$$

to precondition the integral equations for the Laplace operator. Hereabove, the operator K is the double-layer potential operator which is of order -1, K^{T} designates the transposed operator of K and I is the identity operator. Since K is a compact operator of order -1, an appropriate choice of a preconditioner for the exact operator V (respectively N) is the operator N of opposite order (respectively V) in the TM case (respectively TE case) up to a compact perturbation. This idea has been intensively studied by Christiansen and Nédélec [12, 13] for both the Helmholtz and Maxwell's equation. We refer to their papers and do not develop this method here. In practice, the compact part may not be negligible in certain situations as for instance for the propagative modes in the case of a circular cylinder (the relation seems to hold only for the evanescent modes) or for an open surface where there is a loss of compacity of K. If we set $C = VN$, then from a discrete point of view, the spectrum of $[C]$ has an accumulation point at $\frac{1}{4}$ for both the propagative and evanescent modes (cf. Figure 1). This eigenvalues clustering represents an interesting characteristic to provide a faster convergence of a Krylov iterative solver. The correction of the behaviour of the integral equation to solve for the propagative modes by obtaining a zeroth-order operator implies that the linear dependence

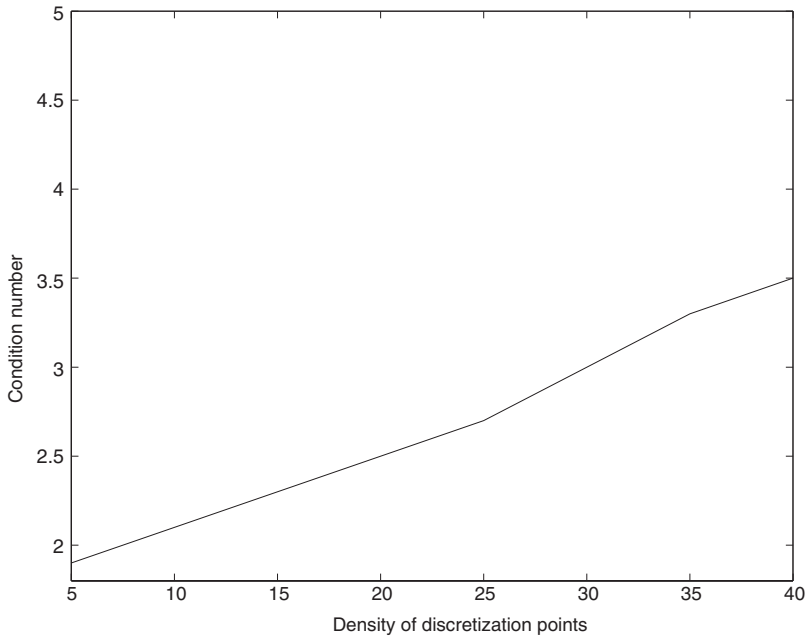

Figure 2. Dependence of the condition number $\kappa([C])$ with respect to n_λ ($D = 10$ and $d = 2$).

of the condition number according to the density of discretization points n_λ is greatly reduced (see Figure 2). However, we can observe the existence of two eigenvalues related to the resonances phenomena of the low-order propagative modes at the endpoints of the strip. This is the second penalizing effect appearing in the analysis of Chew and Warnick and translating the dependence of the condition number according to $D^{1/2}$.

4.2. A new local implicit analytic preconditioner

One of the drawbacks of the explicit integral preconditioners is that the number of MV products per iteration is doubled. In the sequel, the quantity MV will be considered as a good measure of the convergence rate of our iterative solver. Indeed, the main cost in the iterative algorithm is due to the computational complexity needed for these MV evaluations (typically $\mathcal{O}(n^2)$ or $\mathcal{O}(n \log n)$ in the best case using a FMM). Since our goal is to reduce the number of MV products, we propose here to construct a local implicit analytic preconditioner for the EFIE which allows to suppress this problem. Its discretization is realized by a finite element method and leads to the resolution of a small and highly sparse linear system.

4.2.1. TM polarization. Let us recall that the TM–EFIE is given by the following problem: find the density $p = [\partial_{\mathbf{n}} u]_\Gamma$ satisfying: $Vp = g$. To fix the notations, we consider the particular case of the strip $\Gamma = [-1, 1]$. Let us introduce Ω_l as the thin layer defined by $\Omega_l = [-(1 + hl), (1 + hl)] \times [-hl, hl]$, $l \in \mathbb{N}^*$ and h is the uniform meshsize of the boundary element method. Integer l designates the number of layers surrounding Γ and allows a control of the size of Ω_l. Since the spatial discretization step h is fixed to λ/n_λ in the boundary element

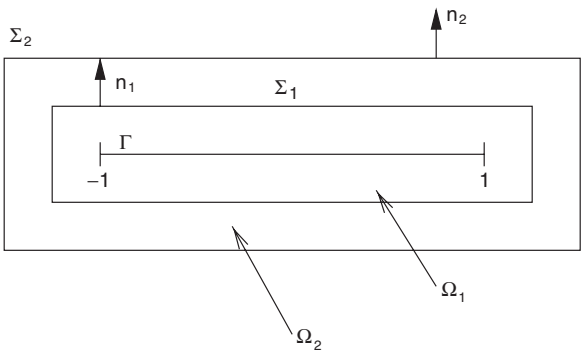

Figure 3. Rectangular layers Ω_l of boundary Σ_l surrounding the strip $\Gamma = [-1, 1]$.

method, the involved computational domain Ω_l is very thin (a fraction of the wavelength). In the sequel, we use the notation $\mathbf{n}_l$ for the outwardly directed unit normal vector to Ω_l at the fictive boundary Σ_l (see Figure 3).

Now, let us assume that we want to construct an approximate solution to the Dirichlet problem. One possible solution is to use an integral equation as the EFIE, but another well-known approach consists in imposing an Absorbing Boundary Condition on a fictive boundary surrounding the scatterer [17–19] and next to solve the resulting bounded BVP by a FEM [20, 21]. To this end, let us suppose that the exact Dirichlet–Neumann (DN) operator Λ^+ [17] is set on the exterior boundary Σ_l of Ω_l. Then we have to solve the following truncated BVP:

$$\begin{aligned} &\text{Find } w \text{ such that} \\ &\Delta w + k^2 w = 0 \quad \text{in } \Omega_l \\ &w_{|\Gamma} = g \quad \text{on } \Gamma \\ &\partial_{\mathbf{n}_l} w + \Lambda^+ w = 0 \quad \text{on } \Sigma_l \end{aligned} \tag{16}$$

Since the DN operator is an exact restriction operator, then the solution w to (16) exactly gives the restriction of u to the domain Ω_l. In some meaning, the DN operator Λ^+ is the exact inverse operator of V. However even if the approach seems optimal at first sight, the *non-local* nature of the DN operator yields to the involvement after discretization of a dense linear system to inverse similarly to the integral equation approach. To remove this limitation, we rather use a localization of the operator Λ^+ in the high-frequency regime leading to a discrete sparse linear system to solve. We choose here to use the mth order ($m \in \mathbb{N}^*/2$) local non-reflecting boundary operators $\mathscr{P}_m(s, \partial_s)$ on Σ_l developed in Reference [17]

$$\partial_{\mathbf{n}_l} w + \mathscr{P}_m(s, \partial_s) w = 0 \quad \text{on } \Sigma_l \tag{17}$$

variable s denoting the anticlockwise directed curvilinear abscissa along Γ. The half-order operator is simply given by the Sommerfeld radiation condition with $\mathscr{P}_{1/2} = -\mathrm{i}k$ and the second-order

one is given by

$$\partial_{\mathbf{n}} w - \left(\mathrm{i}k - \frac{c}{2} + \frac{c^2}{8(\kappa - \mathrm{i}k)} \right) w - \partial_s \left[\frac{1}{2(c - \mathrm{i}k)} \partial_s w \right] = 0 \quad \text{on } \Sigma_l \tag{18}$$

This last condition is also called the second-order symmetrical Bayliss–Gunzburger–Turkel-like ABC [17, 18, 20, 21] and has proved to be efficient in acoustic scattering calculations [20]. Function $c = c(s)$ stands for the curvature at point $s \in \Sigma_l$. Then, setting (17) on the exterior boundary Σ_l, the approximate BVP under consideration is now

$$\begin{aligned} &\text{Find } w \text{ such that} \\ \Delta w + k^2 w &= 0 \quad \text{in } \Omega_l \\ w_{|\Gamma} &= g \quad \text{on } \Gamma \\ \partial_{\mathbf{n}_l} w + \mathscr{P}_m(s, \partial_s) w &= 0 \quad \text{on } \Sigma_l \end{aligned} \tag{19}$$

This gives rise to an approximation w of the solution u restricted to Ω_l. At this level, several remarks must be made. Firstly, the involvement of the ABC allows to reproduce the outgoing character of the reflected wave to the scatterer. Roughly speaking, the construction of the ABC well models the propagative part of the scattered field. Now, since we consider a thin layer surrounding the strip, we should *a priori* consider the creeping waves (given by the frequencies such that $k \approx |\xi|$) to the surface of the flat screen. This is one of the important aspect for the construction of a suitable preconditioner. Finally, since we can control the size of the computational domain by the number l of layers, increasing l should also gives rise to a better modelling of the evanescent part of the reflected wave and should yield a correction to the deterioration linked to the density of points if it is considered in a preconditioner.

Considering the BVP (19), we can now describe how to construct a local implicit analytic preconditioner $\tilde{\mathscr{B}}$ for the TM–EFIE such that $[\partial_{\mathbf{n}} w]_\Gamma = \tilde{\mathscr{B}} g$ by using two successive variational formulations. Next approximated by a FEM, this preconditioner will be denoted by ABC–FEM-based preconditioner.

Step 1: Computation of w on Ω_l: Let us begin by computing the approximate solution w on Ω_l. To this end, we consider a smooth enough test-function φ such that $\varphi_{|\Gamma} \equiv 0$. Using the Green's formula, we obtain,

$$-\int_{\Omega_l} (\Delta w + k^2 w)\varphi \, \mathrm{d}\Omega_l = -\int_{\partial\Omega_l} \partial_{\mathbf{n}} w \varphi \, \mathrm{d}\partial\Omega_l + \int_{\Omega_l} (\nabla w \cdot \nabla \varphi - k^2 w \varphi) \, \mathrm{d}\Omega_l \tag{20}$$

Since we have $\partial\Omega_l = \Sigma_l \cup \Gamma$ and $\varphi_{|\Gamma} \equiv 0$, this last relation yields using (17)

$$-\int_{\Omega_l} (\Delta w + k^2 w)\varphi \, \mathrm{d}\Omega_l = \int_{\Sigma_l} \mathscr{P}^m(s, \partial s) w \varphi \, \mathrm{d}\Sigma_l + \int_{\Omega_l} (\nabla w \cdot \nabla \varphi - k^2 w \varphi) \, \mathrm{d}\Omega_l = 0 \tag{21}$$

Since the ABC is symmetrical in the sense of the $L^2(\Sigma_l)$ scalar product, the integral term can be symmetrized. This direct computation allows us to determine the unknown field w not only on the whole computational domain Ω_l but also on the fictive boundary Σ_l. From a discrete point of view, the approximate solution w is computed by the use of a $\mathbb{P}_1$ Galerkin finite element method. This implies that we have to solve a linear system defined by a small

and sparse symmetrical complex-valued matrix. Concerning the mesh, one requires that each boundary point of Γ of the triangular volume mesh for the scatterer can be exactly connected to one of the surface mesh. So, there is an interconnection between the two meshes, the volume mesh being constructed by a need to satisfy a boundary constraint fixed by the *a priori* known surface mesh.

Step 2: Computation of the density $[\partial_{\mathbf{n}} w]_\Gamma$: To determine the density $[\partial_{\mathbf{n}} w]_\Gamma$, we now choose a test-function φ such that $\varphi_{|\Gamma} \neq 0$. The Green's formula gives the weak formulation

$$-\int_{\Omega_l} (\Delta w + k^2 w)\varphi \, \mathrm{d}\Omega_l = -\int_\Gamma \partial_{\mathbf{n}} w \varphi \, \mathrm{d}\Gamma - \int_{\Sigma_l} \partial_{\mathbf{n}_l} w \varphi \, \mathrm{d}\Sigma_l + \int_{\Omega_l} (\nabla w \cdot \nabla \varphi - k^2 w \varphi) \, \mathrm{d}\Omega_l \tag{22}$$

A more explicit version of this last equation is given by

$$\int_\Gamma \partial_{\mathbf{n}} w \varphi \, \mathrm{d}\Gamma = \int_{\Sigma_l} \mathscr{P}^m(s, \partial s) w \varphi \, \mathrm{d}\Sigma_l + \int_{\Omega_l} (\nabla w \cdot \nabla \varphi - k^2 w \varphi) \, \mathrm{d}\Omega_l \tag{23}$$

However, we have the following sequence of equalities:

$$\int_\Gamma \partial_{\mathbf{n}} w \varphi \, \mathrm{d}\Gamma = \int_\Gamma (\partial_{\mathbf{n}} w)^- \varphi \, \mathrm{d}\Gamma - \int_\Gamma (\partial_{\mathbf{n}} w)^+ \varphi \, \mathrm{d}\Gamma = \int_\Gamma [\partial_{\mathbf{n}} w]_\Gamma \varphi \, \mathrm{d}\Gamma \tag{24}$$

As a consequence, a possible construction of a sparse preconditioner $\tilde{\mathscr{B}}$ is given by using the approximate solution w computed in the first step and using the identification

$$\int_\Gamma \tilde{\mathscr{B}} g \varphi \, \mathrm{d}\Gamma = \int_{\Omega_l} (\nabla w \cdot \nabla \varphi - k^2 w \varphi) \, \mathrm{d}\Omega_l + \int_{\Sigma_l} \mathscr{P}^m(s, \partial_s) w \varphi \, \mathrm{d}\Sigma_l \tag{25}$$

Since the construction of $\tilde{\mathscr{B}}$ requires the solution of a sparse linear system in the first step, then this local preconditioner is of *implicit*-type.

4.2.2. TE polarization. For the TE–EFIE, the construction is similar and the approximate BVP to solve takes into account the Neumann data. The first step may be written under the form,

$$\int_{\Sigma_l} \mathscr{P}^m(s, \partial s) w \varphi \, \mathrm{d}\Sigma_l + \int_{\Omega_l} (\nabla w \cdot \nabla \varphi - k^2 w \varphi) \, \mathrm{d}\Omega_l = -\int_\Gamma g w \varphi \, \mathrm{d}\Gamma \tag{26}$$

for a test-function φ such that $\varphi_{|\Gamma} \neq 0$. From a discrete point of view, we use a $\mathbb{P}_1$ Galerkin finite element method to compute the approximate solution w. The first step still requires the solution to a sparse linear system. We do not develop the details which can be drawn from the preceding case.

4.3. Numerical results for the strip

We now test the efficiency of the preconditioner in the EFIE formulation for the two polarizations for the model strip of Section 4.2.1. For comparisons, we also consider the integral Calderòn preconditioners for each case. Two different Krylov iterative solvers will be tested: the conjugate gradient squared (CGS) and the GMRES(r) algorithms [5], where r designates

the restart parameter. We recall that the CGS method requires two MV products per iteration whereas the GMRES approach only needs one MV product. The implementation of the considered preconditioner $\tilde{\mathscr{B}}$ simply involves in each MV product $\mathbf{y} = [V]\mathbf{x}$ in the initial algorithm by the two successive steps $\tilde{\mathbf{x}} = \tilde{\mathscr{B}}\mathbf{x}$ and next $\mathbf{y} = [V]\tilde{\mathbf{x}}$. We choose a stopping criterion on the relative error for the usual $\|\cdot\|_2$-norm,

$$\frac{\|[V]\mathbf{p}_j - \overline{\mathbf{g}}\|_2}{\|\overline{\mathbf{g}}\|_2} \leqslant \varepsilon \tag{27}$$

where $\overline{\mathbf{g}}$ is the vectorial representation of the boundary element approximation of g involving in the EFIE formulation, vector $\mathbf{p}_j$ is the approximation of p at the jth iteration of the iterative algorithm and ε is an *a priori* fixed tolerance. The incident signal is a plane wave of the form,

$$u^{\text{inc}}(x) = \exp(-\mathrm{i}k(\cos(\theta_0)x_1 + \sin(\theta_0)x_2)) \tag{28}$$

where θ_0 is the incidence angle of the wave in the $\mathbb{R}^2$-plane and (x_1, x_2) are the cartesian co-ordinates of a point x.

As it has been noticed in Section 3, the condition number $\kappa([V])$ of the boundary element matrix $[V]$ essentially depends on two parameters: the high-frequency parameter $D = k/\pi$ and the density of discretization points n_λ. These terms have a direct impact on the convergence rate of the iterative methods. Indeed, if one considers for instance the CGS algorithm, a well-known fact is that the number of iterations $n_{\text{CGS}}^{\text{iter}}$ required to obtain a relative error less than ε may be estimated by

$$n_{\text{CGS}}^{\text{iter}}([V]) \simeq \kappa^{1/2}([V])\,\frac{|\ln(\varepsilon/2)|}{2} \tag{29}$$

Let us analyse the effect of these two parameters on the number of MV products to attain the tolerance $\varepsilon = 10^{-4}$ for the EFIE with the mass matrix as preconditioner, with the Caldèron's preconditioner and finally with the new proposed preconditioner.

In Figures 4 and 5, we draw the dependence of the number of MV products involving, respectively, in the GMRES(50) and CGS algorithms according to the wave number $k = \pi D$ for a density of discretization points $n_\lambda = 20$ and a zero incidence angle for the TM polarization. As it can be observed, the high-frequency dependence of the number of MV products (equal to 10 and 16 with the use of, respectively, the GMRES(50) and CGS solvers) vanishes with the use of the Caldèron operator. We can explain this result as follows. Firstly, the normal derivative of the double-layer potential regularizes the elliptic part of the spectrum of the single-layer potential for the evanescent modes and leads to the accumulation point $1/4$ which is both independent of the wavelength and density of discretization points. Moreover, for the creeping modes, we can see from formulae (8) and (13) that there is a kind of compensation by multiplying the smallest and largest eigenvalues respectively of V and N. In the case of the strip, even if V and N are non-normal, they are almost non-normal since their respective non-normal parts are in a certain sense bounded according to D [7]. This partially explains why we obtain this kind of behaviour. A better behaviour is also observed with the ABC–FEM-based preconditioner and especially when the order l of layers for the preconditioner is increased. We do not really obtain an independent number of MV products according to k but this is almost attained by increasing the number of layers. This can be related to the fact that evanescent modes are better computed with a larger domain. The independence of the number of MV products with both n_λ and D

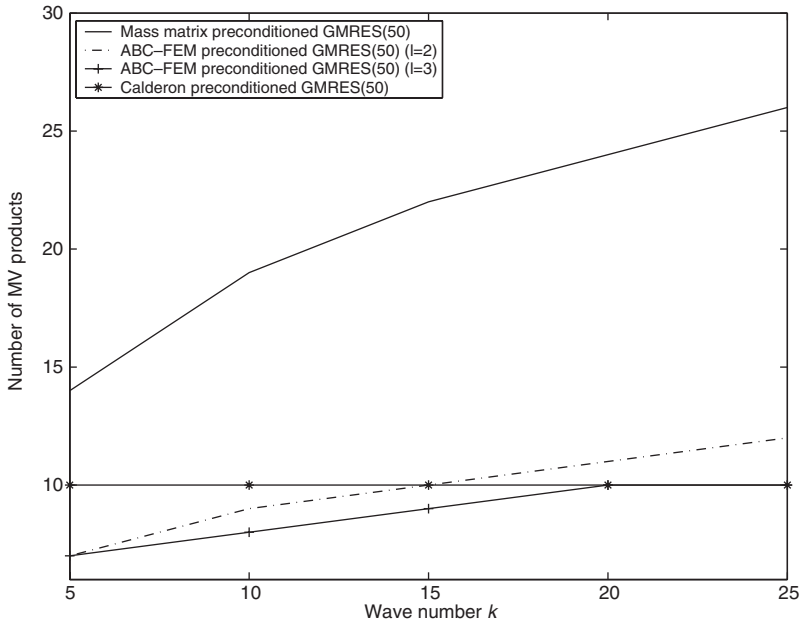

Figure 4. TM polarization for the screen (GMRES): behaviour of the number of MV products according to the wave number k ($n_\lambda = 20,\ \theta_0 = 0°,\ \varepsilon = 10^{-4}$).

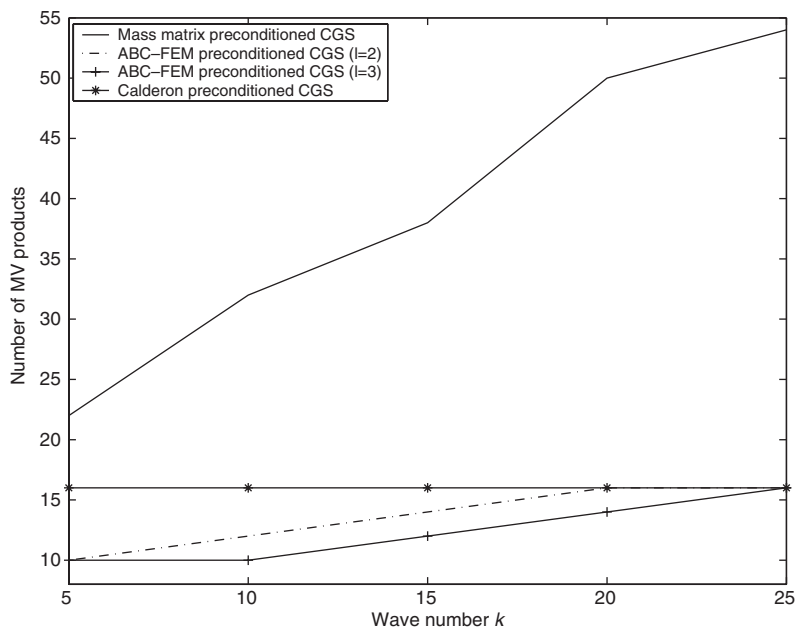

Figure 5. TM polarization for the screen (CGS): behaviour of the number of MV products according to the wave number k ($n_\lambda = 20,\ \theta_0 = 0°,\ \varepsilon = 10^{-4}$).

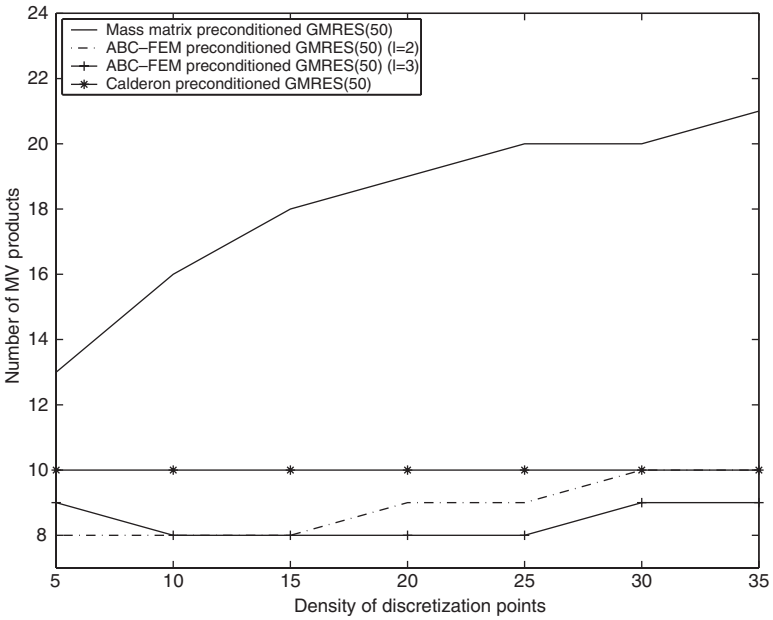

Figure 6. TM polarization for the screen: behaviour of the number of MV products according to n_λ ($k = 10$, $\theta_0 = 0°$, $\varepsilon = 10^{-4}$).

would be attained in the case of more layers but this also increases the computational cost at each iteration of the algorithm which is $\mathcal{O}(n)$ with a constant depending on l. We have used here the GMRES(50) solver accelerated by an incomplete LU preconditioned GMRES(50) for solving the sparse linear system involving in the construction of the preconditioner. We have fixed a tolerance ε equal to 10^{-6}. This resolution has the significant advantage to only require a few number of iterations. In Figure 6, we rather analyse the dependence of the number of MV products according to the density of discretization points for $k = 10$ and $\theta_0 = 0°$. We get an independence of the Calderon preconditioner according to n_λ. As noticed above, this is due to the regularizing effect of the double-layer potential N in the elliptic part of the integral operator V. A better behaviour is given by the ABC–FEM-based preconditioner. We have also observed that the number of MV products is independent of the angle of incidence. Now concerning the order m of the ABC, no improvement has been observed concerning the interest of considering a second-order ABC. It seems that the essential information is embedded in the Sommerfeld condition translating the outgoing character of the scattered field. This is radically different from the results obtained in References [20, 21] in the framework of ABC on a much larger computational domain. Finally, let us notice that no error analysis has been reported here. Indeed, the application of the preconditioner does not influence the accuracy of the boundary element solution.

Let us now consider the TE case. We represent in Figures 7 and 8 the number of MV products involving, respectively, in the GMRES(50) and the CGS algorithms preconditioned by the mass matrix, with the ABC–FEM preconditioner and finally with the single-layer potential according

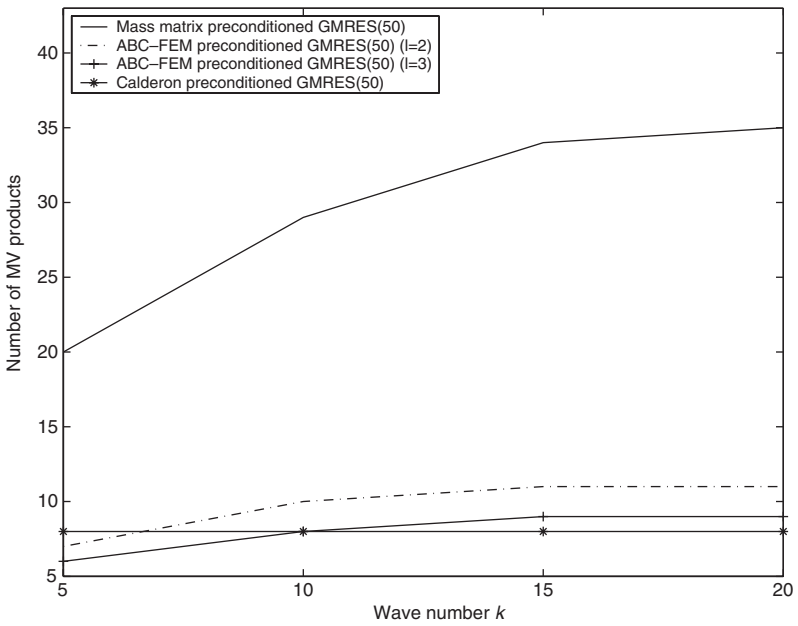

Figure 7. TE polarization for the screen (GMRES): behaviour of the number of MV products according to the wave number k ($n_\lambda = 20$, $\theta_0 = 45°$, $\varepsilon = 10^{-3}$).

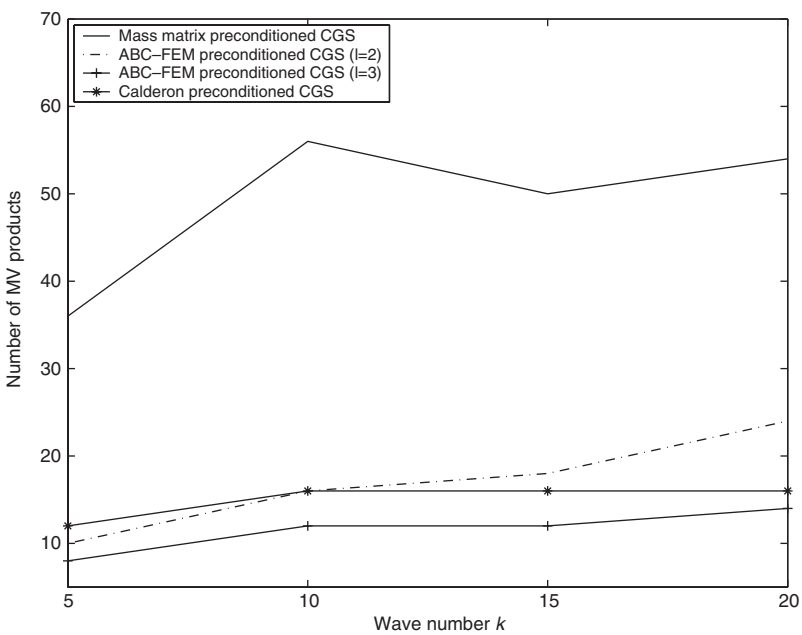

Figure 8. TE polarization for the screen (CGS): behaviour of the number of MV products according to the wave number k ($n_\lambda = 20$, $\theta_0 = 45°$, $\varepsilon = 10^{-3}$).

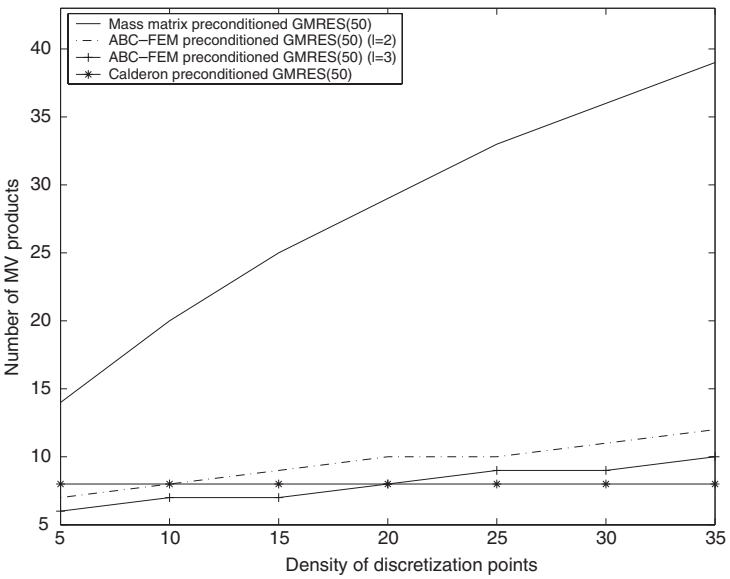

Figure 9. TE polarization for the screen: behaviour of the number of MV products according to n_λ ($k = 10$, $\theta_0 = 45°$, $\varepsilon = 10^{-3}$).

to the wave number k (for $n_\lambda = 20$). In Figure 9, we draw the density of discretization points n_λ for $k = 10$. The angle of attack is fixed to 45° and the tolerance to $\varepsilon = 10^{-3}$. Once again, the improvement induced by the local analytic preconditioner is clear. A better behaviour is achieved at a reduced computational cost handling three layers of finite elements. The underlying physics is incorporated providing a robust preconditioner where the influence of both the electrical size D of the scatterer and the discretization density n_λ of the mesh is substantially reduced on the convergence rate of the Krylov iterative solver.

For any preconditioner or polarization, we remark that the GMRES(50) algorithm yields the smallest number of MV products. In the sequel, we restrict our numerical experiments to the GMRES method (with $r = 50$). Moreover, since the number of layers $l = 3$ seems to represent the best alternative, we only consider this value for all the following tests.

5. EXTENSIONS AND IMPROVEMENTS

We provide in this section two improvements of the ABC–FEM-based preconditioner. The first one consists to test the robustness of the preconditioner in the case of the rectangular cavity where some physical resonant modes strongly affect the convergence rate of the iterative solver applied to the EFIE. The second issue concerns the possibility of localizing the analytic preconditioner by using a domain decomposition of the complete scatterer in the case of a large-size object. We show that in both cases, penalizing scattering effects can be taken into account in the preconditioner by a suitable geometrical decomposition of the scatterer.

5.1. The rectangular resonant cavity

The rectangular cavity consists in two perfectly conducting strips Γ_1 and Γ_2 of width d, separated by a distance w. Let us introduce the dimensionless length $W = w/\lambda$. The particularity of this configuration comes from the presence of resonant modes subsisting in the cavity. They correspond to low-order propagative modes and give rise to small eigenvalues. Consequently, the discrete matrices become ill-conditioned at these resonances. Chew and Warnick [7], provide the following high-frequency estimates of these smallest eigenvalues for, respectively, the TM and TE polarizations:

$$\Lambda_m([V]) \simeq \frac{\mathrm{i}\lambda\sqrt{W}\alpha}{4\pi D}, \quad \Lambda_m([N]) \simeq -\frac{\mathrm{i}\pi\sqrt{W}\alpha}{\lambda D} \tag{30}$$

where α is the fractional part of $2W$. They also prove that the largest eigenvalues are identical to the ones computed for the simple flat strip, i.e. (8) and (12). As a consequence, for $D \to \infty$, the following estimates of the condition numbers hold for the TM and TE polarizations:

$$\kappa([V]) \simeq \frac{4}{3}\frac{D^{3/2}}{\alpha\sqrt{W}}, \quad \kappa([N]) \simeq \frac{n_\lambda D}{2\alpha\sqrt{W}} \tag{31}$$

Moreover, it can be proved that the condition numbers become maximal near the resonances. Sharper estimates are given by

$$\kappa([V]) \simeq \frac{16}{3}\frac{D^{7/2}}{W^{3/2}}, \quad \kappa([N]) \simeq \frac{2n_\lambda D^3}{W^{3/2}} \tag{32}$$

The configuration for the numerical tests is the following. We consider the strip Γ_1 of endpoints $(-1, 0)$ and $(1, 0)$ and the strip Γ_2 of endpoints $(-1, w)$ and $(1, w)$. The Caldèron integral preconditioner is constructed by considering the matrix associated to the domain $\Gamma_1 \cup \Gamma_2$. There is no decoupling between the interaction of the two segments. Numerical tests have been performed to analyse this decoupling effect in the efficiency of the preconditioner. However, poor improvement concerning the convergence rate of the iterative solver compared to the use of the mass matrix has been obtained. This seems linked to the fact that the integral operators modelling the scattering effects are global. Applying the method described in the previous section, we construct the preconditioner $\tilde{\mathscr{B}}_j$ relative to the EFIE sets on Γ_j. The global EFIE matrix is preconditioned by decoupling the two strips considering the block diagonal matrix: $\tilde{\mathscr{P}} = \mathrm{diag}_{1 \leqslant j \leqslant 2}(\tilde{\mathscr{B}}_j)$. Unlike the integral preconditioner, the local character of the ABC–FEM preconditioner allows a decoupling of the structure. As it can be observed in Figures 10–13, a good convergence rate is provided. This is an important feature of the new preconditioner since the decoupling procedure leads to a reduced computational cost. Concerning the efficiency of the method, we obtain a better convergence with only two layers than by using the mass matrix or the Caldèron integral operator as preconditioner. This is confirmed for the two polarizations. As for the strip, the dependence according to both the high-frequency parameter D and the density of discretization points n_λ is weakened. Moreover, we can notice that the complex resonance effects are partially taken into account in the formulation. Once again on this example, the robustness of the local preconditioner is shown.

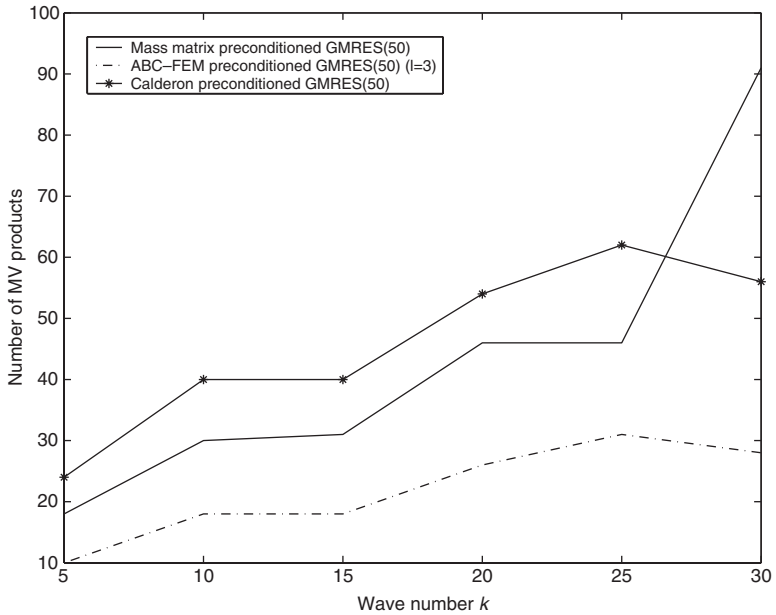

Figure 10. TM polarization for the rectangular cavity: behaviour of the number of MV products according to the wave number k ($w = 0.3$, $n_\lambda = 20$, $\theta_0 = 45°$, $\varepsilon = 10^{-4}$).

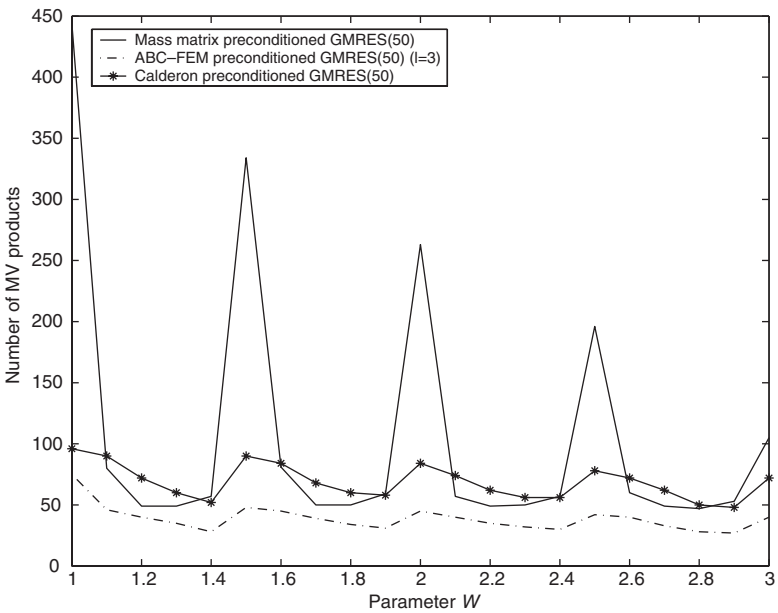

Figure 11. TM polarization for the rectangular cavity: behaviour of the number of MV products according to the cavity dimension W ($D = 10$, $n_\lambda = 10$, $\theta_0 = 45°$, $\varepsilon = 10^{-4}$).

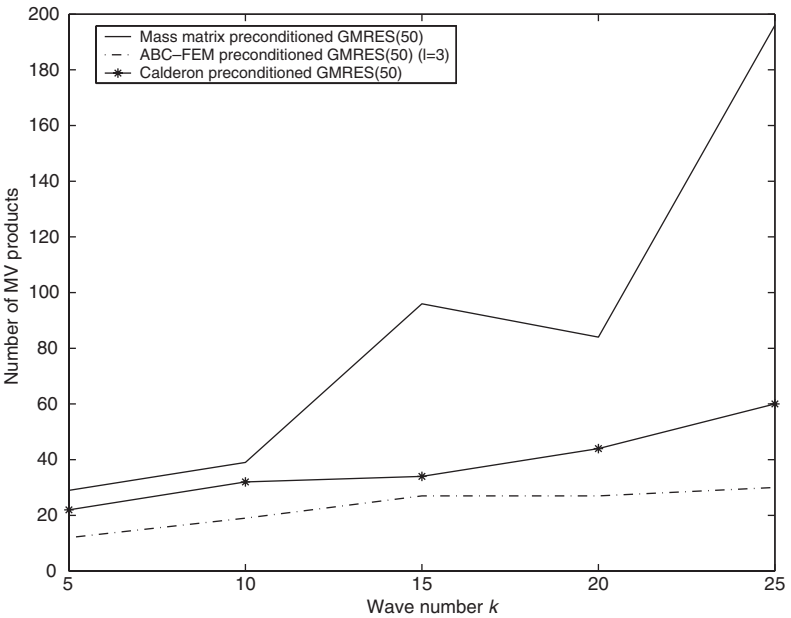

Figure 12. TE polarization for the rectangular cavity: behaviour of the number of MV products according to the wave number k ($n_\lambda = 20$, $\theta_0 = 45°$, $\varepsilon = 10^{-3}$).

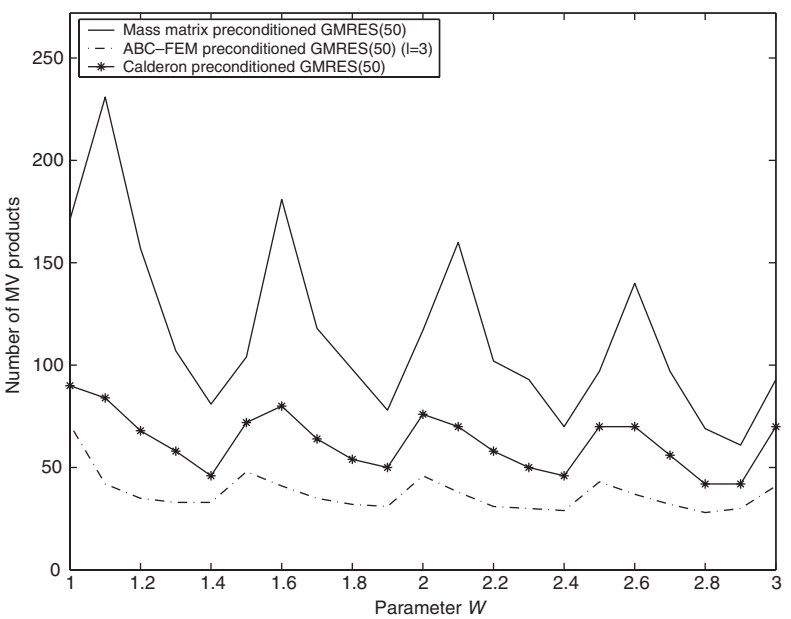

Figure 13. TE polarization for the rectangular cavity: behaviour of the number of MV products according to the cavity dimension W ($D = 10$, $n_\lambda = 10$, $\theta_0 = 45°$, $\varepsilon = 10^{-3}$).

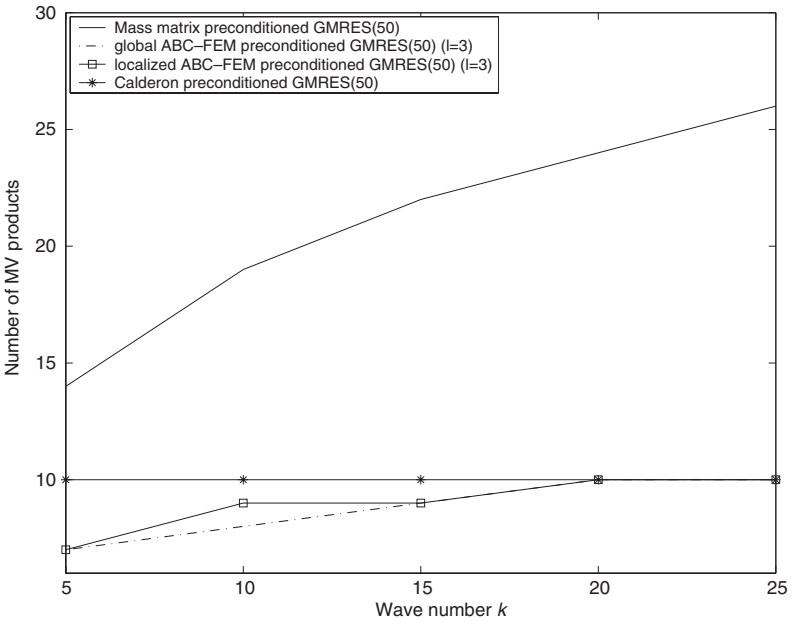

Figure 14. Effect of the domain decomposition (TM polarization): behaviour of the number of MV products according to k ($n_\lambda = 20$, $\theta_0 = 0°$, $\varepsilon = 10^{-4}$).

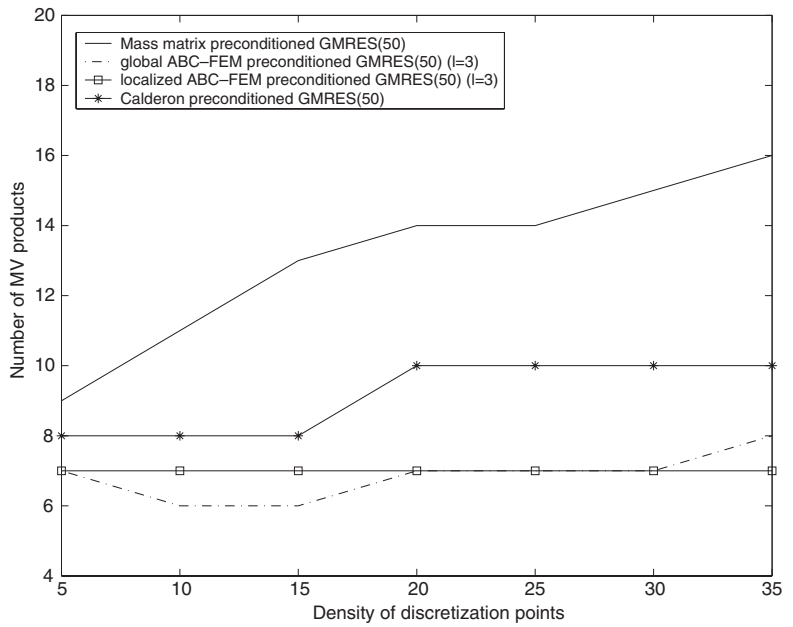

Figure 15. Effect of the domain decomposition (TM polarization): behaviour of the number of MV products according to n_λ ($k = 5$, $\theta_0 = 0°$, $\varepsilon = 10^{-4}$).

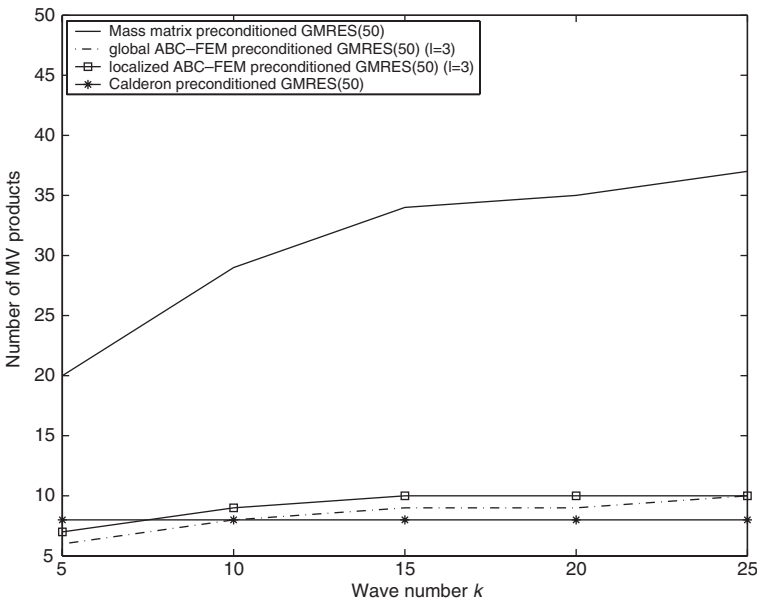

Figure 16. Effect of the domain decomposition (TE polarization): behaviour of the number of MV products according to k ($n_\lambda = 20$, $\theta_0 = 45°$, $\varepsilon = 10^{-3}$).

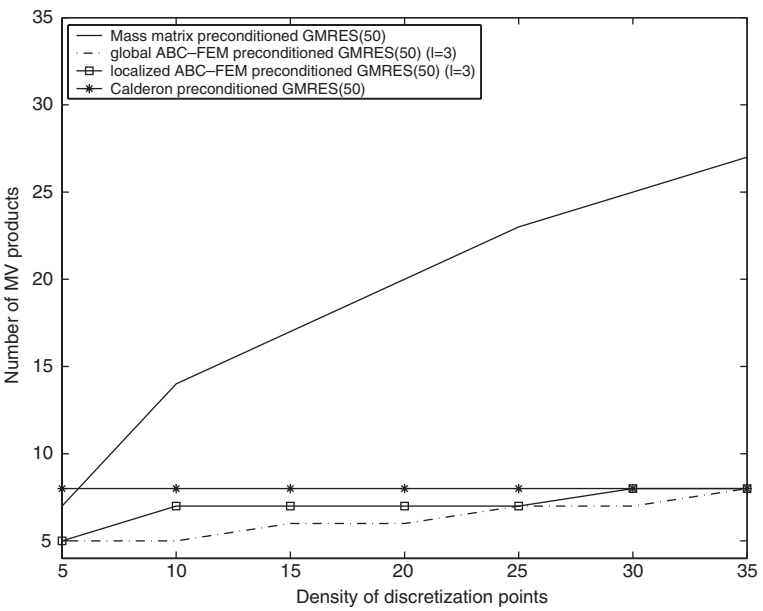

Figure 17. Effect of the domain decomposition (TE polarization): behaviour of the number of MV products according to n_λ ($k = 5$, $\theta_0 = 45°$, $\varepsilon = 10^{-3}$).

5.2. A domain partitioning procedure for the localization of the ABC–FEM preconditioner

The efficiency of the ABC–FEM-based preconditioner has been shown on two problems: the screen and the rectangular cavity. However, when one considers a large electrical structure in high-frequency, it can be interesting to partition the global domain into a set of smaller structures. The goal is to localize the linear system to inverse into smaller block diagonal sparse matrices faster to solve. To illustrate the method, we consider again the particular case of the strip $\Gamma = [-1, 1]$. We decompose Γ into two smaller screens $\Gamma_1 = [-1, h]$ and $\Gamma_2 = [-h, 1]$. As it can be noticed, there is a small overlapping domain connecting the two domains. Next, we consider some test-functions for the left (respectively right) screen such that they vanish at the right endpoint $(h, 0)$ (respectively the left endpoint $(-h, 0)$). This permits to have a decoupled partitioning of the scatterer and to construct each preconditioner $\tilde{\mathscr{B}}_j$ relative to each domain Γ_j. Following this strategy, we can precondition the linear system associated to this configuration with the block-diagonal matrix $\tilde{\mathscr{P}} = \mathrm{diag}_{1 \leqslant j \leqslant 2}(\tilde{\mathscr{B}}_j)$. For comparisons, we also give the results for the mass matrix preconditioner, the global Caldèron integral preconditioner and the ABC–FEM for the whole structure Γ. We can see in Figures 14–17 that the convergence rate is not really affected by the domain decomposition of the strip and similar results are obtained for both polarizations. The partitioning strategy provides a convergence rate which is better than by using the other kinds of preconditioners.

6. CONCLUSION

We have proposed in this paper a new local implicit analytic preconditioner for the EFIE. The method is based on the resolution of the Helmholtz equation in a thin domain truncated with an artificial boundary condition. The preconditioner includes some corrections linked to both the physics, geometry and boundary element approximation which affect the conditioning of the linear system associated to the boundary element approximation of the EFIE. The efficiency of this preconditioner has been tested for the scattering problem by some open surfaces (flat strip and resonant cavity). Moreover, in the case of a large electrical size scatterer, a domain decomposition method of the target can be developed to speed up the preconditioning strategy of the system. Finally, comparisons with both the classical mass matrix preconditioner and Caldèron integral preconditioners have been provided. To confirm the analysis and efficiency of the preconditioner, three-dimensional calculations for the EFIE associated to the Maxwell's equation still remain to do. However, this aspect is beyond the scope of the present paper and further investigations must be developed.

REFERENCES

1. Colton D, Kress R. Integral equation methods in scattering theory. *Pure and Applied Mathematics.* Wiley: New York, 1983.
2. Chew WC, Jin JM, Michielssen E, Song J. *Fast and Efficient Algorithms in Computational Electromagnetics.* Artech House Antennas and Propagation Library: Norwood, 2001.
3. Rokhlin V. Rapid solution of integral equations of scattering theory in two-dimensions. *Journal of Computational Physics* 1990; **186**:414–439.
4. Amini S, Maines ND. Preconditioned Krylov subspace methods for boundary element solution of the Helmholtz equation. *International Journal for Numerical Methods in Engineering* 1998; **41**:875–898.
5. Saad Y. *Iterative Methods for Sparse Linear Systems*. PWS Pub. Co.: Boston, 1996.

6. Darve D. The fast multipole method: numerical implementation. *Journal of Computational Physics* 2000; **160**(1):195–240.
7. Chew WC, Warnick KF. On the spectrum of the electric field integral equation and the convergence of the moment method. *International Journal for Numerical Methods in Engineering* 2001; **51**:475–489.
8. Chen K. On a class of preconditioning methods for dense linear systems from boundary elements. *SIAM Journal on Scientific Computing* 1998; **20**:684–698.
9. Carpentieri B, Duff IS, Giraud L. Experiments with sparse approximate preconditioning of dense linear problems from electromagnetic applications. *Technical Report TR/PA/00/04*, CERFACS, France, 2000.
10. Carpentieri B, Duff IS, Giraud L. Sparse pattern selection strategies for robust Frobenius norm minimization preconditioners in electromagnetism. Preconditioning techniques for large sparse matrix problems in industrial applications (Minneapolis, MN, 1999). *Numerical Linear Algebra with Applications* 2000; **7**(7–8):667–685.
11. Chen K. An analysis of sparse approximate inverse preconditioners for boundary elements. *SIAM Journal on Matrix Analysis and Applications* 2001; **22**(4):1958–1978.
12. Christiansen SH, Nédélec JC. Des préconditionneurs pour la résolution numérique des équations intégrales de frontière de l'acoustique. *Comptes Rendus des Seances de l'Academie des Sciences Série I (Mathematique)* 2000; **330**(7):617–622.
13. Christiansen SH, Nédélec JC. Des préconditionneurs pour la résolution numérique des équations intégrales de frontière de l'électromagnétisme. *Comptes Rendus des Seances de l'Academie des Sciences Série I* 2000; **331**(9):733–738.
14. Steinbach O, Wendland WL. The construction of some efficient preconditioners in the boundary element method. *Advances in Computational Mathematics* 1998; **9**(1–2):191–216.
15. Taylor M. *Pseudodifferential Operators.* Princeton University Press: Princeton, NJ, 1981.
16. Darbas M. Préconditionneurs de Type Caldèron pour les Equations Intégrales de l'Electromagnétisme. *Ph.D. Thesis*, Université P. Sabatier, Toulouse, France, 2004, in preparation.
17. Antoine X, Barucq H, Bendali A. Bayliss-Turkel-like radiation conditions on surfaces of arbitrary shape. *Journal of Mathematical Analysis and Applications* 1999; **229**:184–211.
18. Bayliss A, Turkel E. Radiation boundary conditions for wave-like equations. *Communications on Pure and Applied Mathematics* 1980; **23**:707–725.
19. Engquist B, Majda A. Absorbing boundary conditions for the numerical simulation of waves. *Mathematics of Computation* 1977; **31**:629–651.
20. Djellouli R, Farhat C, Macebo A, Tezaur R. Finite element solution of two-dimensional acoustic scattering problems using arbitrarily shaped convex artificial boundaries. *Journal of Computational Acoustics* 2000; **8**:81–100.
21. Tezaur R, Macedo A, Farhat C, Djellouli R. Three-dimensional finite element calculations in acoustic scattering using arbitrarily shaped convex artificial boundaries. *International Journal for Numerical Methods in Engineering* 2002; **53**:1461–1476.

